The Astrophysical Journal, 806:233 (14pp), 2015 June 20 doi:10.1088/0004-637X/806/2/233

DYNAMICAL FIELD LINE CONNECTIVITY IN MAGNETIC TURBULENCE

D. Ruffolo[1] and W. H. Matthaeus[2]
[1] Department of Physics, Faculty of Science, Mahidol University, Bangkok 10400, Thailand; david.ruf@mahidol.ac.th
[2] Bartol Research Institute and Department of Physics and Astronomy, University of Delaware, Newark, DE 19716, USA
Received 2015 January 20; accepted 2015 May 19; published 2015 June 19

ABSTRACT

Point-to-point magnetic connectivity has a stochastic character whenever magnetic fluctuations cause a field line random walk, but this can also change due to dynamical activity. Comparing the instantaneous magnetic connectivity from the same point at two different times, we provide a nonperturbative analytic theory for the ensemble average perpendicular displacement of the magnetic field line, given the power spectrum of magnetic fluctuations. For simplicity, the theory is developed in the context of transverse turbulence, and is numerically evaluated for the noisy reduced MHD model. Our formalism accounts for the dynamical decorrelation of magnetic fluctuations due to wave propagation, local nonlinear distortion, random sweeping, and convection by a bulk wind flow relative to the observer. The diffusion coefficient D_X of the time-differenced displacement becomes twice the usual field line diffusion coefficient D_x at large time displacement t or large distance z along the mean field (corresponding to a pair of uncorrelated random walks), though for a low Kubo number (in the quasilinear regime) it can oscillate at intermediate values of t and z. At high Kubo number the dynamical decorrelation decays mainly from the nonlinear term and D_X tends monotonically toward $2D_x$ with increasing t and z. The formalism and results presented here are relevant to a variety of astrophysical processes, such as electron transport and heating patterns in coronal loops and the solar transition region, changing magnetic connection to particle sources near the Sun or at a planetary bow shock, and thickening of coronal hole boundaries.

Key words: diffusion – magnetic fields – turbulence

1. INTRODUCTION

Magnetic connectivity in simplest terms addresses the question of whether a magnetic field line that passes through a selected point A will also pass, further along its path, through a point B. The physical importance of this connectivity relies on the likelihood that charged particles, especially electrons, may follow the field lines from position A to B, communicating heat flux or energetic particles between the points. One may also envision that a wave energy flux travels along field lines, e.g., for Alfvén waves. To the degree to which field lines act as conduits in this way, connectivity is construed as a factor of substantial importance in astrophysical applications. Suppose that a fiducial (laminar or unperturbed) field line passes through A and B, so they are magnetically connected over a parallel distance z. Then suppose that turbulent fluctuations (or waves) are added to the space between A and B, and the field lines are recomputed according to standard procedures. Since the field lines are distorted by the turbulence, it is likely that the physical points A and B are no longer collocated along a single field line. Instead, the point B' that is connected over a distance z from point A will be separated from point B by a random $\boldsymbol{X}(z)$ (see Figure 1).[3] The degree to which a field line departs from its laminar trajectory, measured by the statistical properties of $\boldsymbol{X}(z)$, is the subject of the theory of the field line random walk (FLRW). Under suitable circumstances this can lead to a type of diffusion away from the fiducial field line (Jokipii 1966; Jokipii & Parker 1968; Matthaeus et al. 1995). A related question is that of two field lines that begin at nearby points A_1 and A_2, each of which is followed for a parallel distance z to positions B_1 and B_2. The statistical distribution of this field line separation $\Delta\boldsymbol{X}_{12}(z)$ is a problem related to the FLRW that has numerous applications as well (Jokipii 1973).

In the above cases the field lines are always calculated from the magnetic field at a single instant of time. Therefore the time dependence of the turbulence is irrelevant for the FLRW and for field line separation as formulated above. However, applications of the idea of magnetic connectivity often involve time variation in an essential way. For example, in the problem of planetary upstream waves, magnetic connection to the bow shock at one instant may or may not imply connection a fixed time later. In the process of diffusive shock acceleration, the probability that a charged particle escapes after a specified time from the acceleration region is related to how long the particle remains magnetically connected to the shock. Likewise, time-varying connectivity may be related to dropouts in observations of solar energetic particles (Mazur et al. 2000; Gosling et al. 2004).

It is clear that a problem may be formulated that involves turbulence evolution in time, and this new problem is readily seen to be relevant to many of the circumstances alluded to above. Our formulation, illustrated in Figure 1, is as follows. Suppose the field line that passes through point A at time t_1 also passes through point B at the same time. Then the points A and B are magnetically connected at time t_1. At a later time $t_2 > t_1$, we again calculate the field line that passes through the same point A, and examine the point B' along that line at the same parallel distance z from point A. This instantaneous field line tracing is well-defined and is physically appropriate when considering the transport of energetic particles that move much faster than the Alfvén speed and sound speed of the plasma. In general we expect that points B and B' will be separated by a random time-differenced displacement $\boldsymbol{X}(z, t = t_2 - t_1)$. In the

[3] The points A and B might also be construed as anchored to material elements, which themselves are mobile. In that case the change of magnetic connectivity between A and B is related to the notion of "general magnetic reconnection," as described for example by Hesse et al. (1990). However for the main part of the discussion here, the points A and B refer to absolute positions in space.

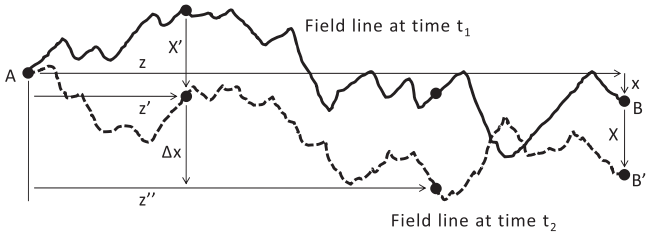

Figure 1. Illustration of magnetic field lines connected to the same point A at time t_1 (thick solid curve) and at time t_2 (thick dashed curve). In this work, we examine field line connectivity by calculating the variance of the displacement $X(z, t)$ between points B and B' along the two field lines as a function of distance z along the mean magnetic field and the time separation $t \equiv t_2 - t_1$. This figure also illustrates some quantities used for deriving the analytic theory.

present work we examine the statistical properties of this time-differenced displacement and an associated diffusion coefficient in the case of transverse magnetic fluctuations. We develop a general analytic expression that depends only on the fluctuation power spectrum and its dynamical correlation, and then consider the results for a model of noisy reduced magnetohydrodynamic (RMHD) turbulence (Ruffolo & Matthaeus 2013).

2. DYNAMICAL FIELD LINE CONNECTIVITY

2.1. Time-differenced Displacement Distribution

Consider a magnetic field $\boldsymbol{B} = \boldsymbol{B}_0 + \boldsymbol{b}$ composed of a large-scale field $\boldsymbol{B}_0$ and a fluctuating component $\boldsymbol{b}(\boldsymbol{x})$ of mean zero. We assume that these random fluctuations are statistically homogeneous in space and time. For simplicity we assume that the fluctuations are transverse, that is, $\boldsymbol{b} \perp \boldsymbol{B}_0$, and that $\boldsymbol{B}_0$ is uniform in space and constant in time. With these assumptions, a field line never backtracks along z, the coordinate along B_0, and the field line trajectory at a single instant of time can be specified by single-valued random functions $x(z)$ and $y(z)$. For brevity we will also denote the perpendicular displacement (x,y) by the vector $\boldsymbol{x}_\perp$. In the present work we examine the dynamical field line connectivity, so we consider two field line trajectories that start from the origin at different times t_1 and t_2, so that $\boldsymbol{x}_\perp(z = 0, t_1) = \boldsymbol{x}_\perp(z = 0, t_2) = 0$. The trajectories within a given realization of $\boldsymbol{b}$ are described by $\boldsymbol{x}_\perp(z, t_1)$ and $\boldsymbol{x}_\perp(z, t_2)$, respectively. Given the assumption of transverse fluctuations, we can uniquely specify these perpendicular displacements at different times for the same parallel displacement z. For simplicity we will also assume axisymmetry, so that statistics of x- and y-displacements are identical at any given time. We will show derivations for quantities along one Cartesian coordinate, say x, which will also apply to those along y. However, the dynamical correlation is not required to be axisymmetric, e.g., when the mean magnetic field and mean flow are not co-linear, and this can lead to nonaxisymmetry in the time-differenced displacement $\boldsymbol{X}$.

It is worth noting that solar wind magnetic fluctuations in the inner heliosphere have been found to be about 90% transverse in terms of fluctuation energy (Belcher & Davis 1971), and there are physical reasons why a large-scale magnetic field $\boldsymbol{B}_0$ can organize turbulent fluctuations to be mostly transverse (Matthaeus et al. 1996). However, such organization would not be expected if the root-mean-squared fluctuation amplitude b greatly exceeds B_0. Our analytic calculations use a non-perturbative framework that does not require the fluctuations to be small, but the assumption of transverse fluctuations will likely become physically unrealistic when $b \gg B_0$. Nevertheless, there are other physical effects that could enhance the transverse components of $\boldsymbol{b}$, such as stratification or rotation.

The calculation of the time-differenced FLRW proceeds as follows. The field line at time t_1 is specified by

$$x(z, t_1) = \frac{1}{B_0}\int_0^z b_x\big[\boldsymbol{x}_\perp(z'), z', t_1\big]dz' \tag{1}$$

and the analogous equation for $y(z, t_1)$. Throughout the paper we use $\langle ... \rangle$ to denote the Reynolds ensemble average. The random walk of the field line has a mean x-displacement of zero (because $\langle b_x \rangle = 0$), but a non-zero, time-independent variance given by

$$\Big\langle x^2(z)\Big\rangle = \frac{1}{B_0^2}\int_0^z \int_0^z \Big\langle b_x\big[\boldsymbol{x}_\perp(z'), z', t_1\big] \times b_x\big[\boldsymbol{x}_\perp(z''), z'', t_1\big]\Big\rangle dz'dz''. \tag{2}$$

Switching z' and z'' as necessary to obtain $z' \leqslant z''$ (for reasons to be explained shortly), we have

$$\begin{aligned}\Big\langle x^2(z)\Big\rangle &= \frac{2}{B_0^2}\int_0^z \int_{z'}^z \Big\langle b_x\big(0, 0, 0\big) \\ &\quad \times b_x\big[\boldsymbol{x}_\perp(z'') - \boldsymbol{x}_\perp(z'), z'' - z', 0\big]\Big\rangle dz''dz' \\ &= \frac{2}{B_0^2}\int_0^z \int_0^{z-z'} \mathcal{L}_{xx}(\Delta z)d\Delta z dz',\end{aligned} \tag{3}$$

where $\Delta z \equiv z'' - z'$ and we invoke spatial and temporal homogeneity. We use the symbol $\mathcal{L}_{xx}(\Delta z)$ with one argument to denote the ensemble average Lagrangian correlation of b_x at two locations offset by distance Δz along the same magnetic field line. This is not to be confused with the Eulerian correlation between the fluctuation at two fixed points. Evaluating Equation (3) is the standard FLRW problem for transverse fluctuations. For recent progress regarding this problem, see Ruffolo & Matthaeus (2013) and references therein.

Now consider displacements $\boldsymbol{x}_\perp(z, t_1)$ for time t_1 and $\boldsymbol{x}_\perp(z, t_2)$ for time t_2. We define the difference between the displacements as $\boldsymbol{X} = (X, Y) \equiv \boldsymbol{x}_\perp(z, t_2) - \boldsymbol{x}_\perp(z, t_1)$, which is a function of z and $t \equiv t_2 - t_1$. The time-differenced x-displacement, denoted by X, has a mean value of zero and a variance given by

$$\begin{aligned}\Big\langle X^2(z, t)\Big\rangle &= \Big\langle \big[x(z, t_2) - x(z, t_1)\big]^2\Big\rangle = \Big\langle x(z, t_1)^2\Big\rangle \\ &\quad - 2\langle x(z, t_1)x(z, t_2)\rangle + \Big\langle x(z, t_2)^2\Big\rangle \\ &= 2\Big\langle x^2(z)\Big\rangle - 2\langle x(z, t_1)x(z, t_2)\rangle,\end{aligned} \tag{4}$$

where the second line follows because the turbulence is considered stationary in time.

The main results of this paper will be to evaluate the expressions in Equation (4) for the mean square separation as a function of distance for two field lines both passing through a known point, but at times separated by the parameter t. Before turning to a detailed description of approximations and models to be employed in the evaluation, we briefly digress concerning expected regimes of behavior of magnetic field line transport in

space and time. This will also enable us to better establish a context of related work.

2.2. Expected Asymptotic and Intermediate Ranges of Behavior

For most types of dynamical fluctuations, e.g., turbulent fluctuations, when the time separation t is sufficiently large, $b_x[\boldsymbol{x}_\perp(z, t_1), z, t_1]$ and $b_x[\boldsymbol{x}_\perp(z, t_2), z, t_2]$ have a negligible correlation for all z, even $z = 0$, and the last term in Equation (4) becomes negligible. Then we obtain $\langle X^2(z, t)\rangle = 2\langle x^2(z)\rangle$ and the problem reduces to the standard FLRW problem, which seeks to determine $\langle x^2(z)\rangle$ (Jokipii & Parker 1968). Furthermore this relation implies a general result applicable at large times t to all cases in which $\langle x^2\rangle$ and $\langle X^2\rangle$ attain diffusive limits, namely that the respective diffusion coefficients are related as

$$\lim_{z\to\infty}\frac{\left\langle X^2(z, t)\right\rangle}{2z} = D_X = 2\lim_{z\to\infty}\frac{\left\langle x^2(z)\right\rangle}{2z} = 2D_x. \qquad (5)$$

This relation becomes intuitively clear whenever $x(z, t_1)$ and $x(z, t_2)$ are uncorrelated because they are separated by a time interval $|t_2 - t_1|$ much greater than a correlation time, so that we are simply determining the difference between uncorrelated random walks. The reasoning here, as well as the result, are closely analogous to the diffusive separation between two random-walking field lines (traced from different locations at the same time) as a function of z, studied originally by Jokipii (1973). Once the separation increases to distances much greater than a coherence length, the mean square separation increases at twice the FLRW rate, in analogy with Equation (5). In these limits initial displacements in either space or time become irrelevant as the two field lines become uncorrelated.

At the other extreme, one readily sees from Equation (4) that if $t = 0$ or $z = 0$ then $X \equiv 0$. For $t = 0$ there is only one field line under consideration so the separation must remain zero at all distances. However for even very small time separations t in dynamical turbulence, the two field lines will respond to different fluctuations, and their asymptotic spatial separation will be the cumulative effect of these differences (Kraichnan 1966; Lundgren 1981). We expect this spatial separation to grow without bound in the diffusive regime. Therefore the $t \to 0$ limit of the asymptotic spatial separation is a singular limit, just as it is for the single time separation problem as the specified spatial separation approaches, but does not equal, zero.

The non-trivial case is for finite time difference t and parallel distance z that are sufficiently small that there is still some correlation between $x(z, t_1)$ and $x(z, t_2)$, so that $0 < \langle X^2(z, t)\rangle < 2\langle x^2(z)\rangle$, and similarly, $0 < \langle Y^2(z, t)\rangle < 2\langle x^2(z)\rangle$. The mathematical formulation here, with time separation as a parameter, is therefore structurally similiar to the mean-squared separation between two field lines that started at different locations (Jokipii 1973). Note that our procedure will be closer to that of Ruffolo et al. (2004).

The mean-squared separation also tends to $2\langle x^2(z)\rangle$, for a long distance z or a large initial separation X_0, because in those cases the two field lines are undergoing independent random walks (except in the case of pure slab fluctuations that have no dependence on the transverse displacement).

The roster of possible intermediate transport regimes is also an interesting topic, and useful in constructing closures in contexts related to the present topic (see, e.g., Rechester & Rosenbluth 1978; Chandran & Cowley 1998), even though the range of scales over which they may be observed is typically confined to a relatively brief transitional phase. In the following sections, our procedures will require adopting a closure assumption, and as preparation for this, we will here briefly review several possibilities. This also permits our presentation to make contact with some related work.

First, as with most transport phenomena, one expects a free streaming regime (Batchelor 1950), in which displacements increase linearly, and the mean square separation $\langle X^2\rangle$ increases quadratically. If the fields are smooth enough, free streaming is always expected at sufficiently small displacements, e.g., smaller than a Kolmogorov dissipation scale, although its range of applicability may evidently extend beyond this in some cases, as we shall presently discuss.

One also frequently encounters the idea of exponentially increasing separations (Rechester & Rosenbluth 1978; Chandran & Cowley 1998; Narayan & Medvedev 2001), a phenomenon traceable to the application of Lyapunov analysis of single scale chaotic dynamical systems (e.g., Zaslavsky & Chirikov 1972). However the applicability of this "stochastic instability" to multiscale systems has been questioned (Ruffolo et al. 2004; Ragot 2008). For example, direct computer simulations of the FLRW indicate that the "exponential" increase in separation often changes to diffusive separation over a distance shorter than the exponential scale length, so that the "exponential" is effectively a linear increase that corresponds to free streaming (Ruffolo et al. 2004).In some cases it has been shown that diffusion theory works better with alternative assumptions (Matthaeus et al. 2003; Ruffolo et al. 2012) concerning the cause of decorrelation in a Green–Kubo–Taylor formulation. Recent results suggest that in a complex system such as flux surfaces in magnetic turbulence (Servidio et al. 2014), the distance between points *measured along the highly corrugated flux surface* may increase exponentially, even as the rectilinear linear separation grows linearly or diffusively ($\sim\sqrt{z}$).

Another familiar regime of intermediate transport, appropriate to the inertial range of spatial separations, is so-called Richardson diffusion, originally formulated for the pair separations of passive tracer particles in hydrodynamics (Richardson 1926; Frisch 1995). Pair separation in a direction indicated by $\boldsymbol{l}$ increases at rate given by the longitudinal velocity increment $\delta u_l = \boldsymbol{l}\cdot[(\boldsymbol{u}(\boldsymbol{x}+\boldsymbol{l}) - \boldsymbol{u}(\boldsymbol{x})]$ where $\mathbf{u}$ is the turbulent velocity and $\boldsymbol{l}$ the separation of the material tracers. The essential physics is to employ the Kolmogorov (1941) estimate of the second order structure function, $\langle u_l^2\rangle = C\epsilon^{2/3}l^{2/3}$, where ϵ is the rate of dispersion of energy per mass, to integrate approximately as $dl/dt = \delta u_l \sim C^{1/2}\epsilon^{1/3}l^{1/3}$ from which $l^2 \sim t^3$. This is a form of superdiffusion that is faster than free streaming. Using heuristic physical arguments analogous to the hydrodynamic passive tracer, the Richardson-like regime for field line transport has been described in a number of papers (e.g., Lazarian & Vishniac 1999; Narayan & Medvedev 2001; Lazarian 2006).

Later in this work, we will employ Corrsin's approximation, which requires a "closure," i.e., an assumption for the variances of displacement distributions, and the closure we employ is based on the transient startup behavior of ballistic spreading.

This is just an input to Corrsin's approximation, not a direct assumption for the resulting expressions for $\langle x^2(z)\rangle$ or $\langle X^2(z, t)\rangle$. Indeed in previous work, the Corrsin-based theory often gave good agreement with direct computer simulations of the FLRW (e.g., Ghilea et al. 2011; Snodin et al. 2013a, 2013b; Sonsrettee et al. 2015) with clear regimes of ballistic, intermediate, and diffusive behavior, regardless of whether we employed a ballistic, diffusive, or self-consistent closure. The situation is analogous to the famous quasilinear approach to energetic particle transport by (Jokipii 1966), who employed unperturbed, helical particle orbits as input to derive a very useful expression for pitch angle diffusion.

2.3. Reduction of Lagrangian to Eulerian Correlations

In analogy with the derivation of the separation between field lines by Ruffolo et al. (2004), we proceed to examine the time-displaced correlation $\langle x(z, t_1)x(z, t_2)\rangle$ in order to determine the full z and t dependence of $\langle X^2(z, t)\rangle$:

$$\langle x(z, t_1)x(z, t_2)\rangle = \frac{1}{B_0^2}\int_0^z \int_0^z \Big\langle b_x\big(\boldsymbol{x}'_{\perp 1}, z', t_1\big) \times b_x\big(\boldsymbol{x}''_{\perp 2}, z'', t_2\big)\Big\rangle dz''dz', \quad (6)$$

where we use the shorthand $\boldsymbol{x}'_{\perp 1} \equiv \boldsymbol{x}_\perp(z', t_1)$, etc. Again, we will find it useful to switch z' and z'' as necessary to obtain $z' \leqslant z''$ and invoke temporal homogeneity, leading to

$$\begin{aligned}\langle x(z, t_1)x(z, t_2)\rangle &= \frac{2}{B_0^2}\int_0^z \int_{z'}^z \frac{1}{2}\Big[\Big\langle b_x\big(\boldsymbol{x}'_{\perp 1}, z', t_1\big) \times b_x\big(\boldsymbol{x}''_{\perp 2}, z'', t_2\big)\Big\rangle \\ &\quad + \Big\langle b_x\big(\boldsymbol{x}'_{\perp 2}, z', t_2\big)b_x\big(\boldsymbol{x}''_{\perp 1}, z'', t_1\big)\Big\rangle\Big]dz''dz' \\ &= \frac{2}{B_0^2}\int_0^z \int_0^{z-z'} \Big\langle b_x(\boldsymbol{x}'_{\perp 0}, z', 0) \times b_x\big(\boldsymbol{x}''_{\perp t}, z'', 0\big)\Big\rangle_\pm d\Delta z dz' \\ &= \frac{2}{B_0^2}\int_0^z \int_0^{z-z'} \mathcal{L}_{xx}(\Delta z, z', t)d\Delta z dz', \end{aligned} \quad (7)$$

recalling that $\Delta z \equiv z'' - z'$ and $t \equiv t_2 - t_1$. Here we use the subscripts "0" and "t" for two times separated by t, we use the subscript "$\pm$" to imply averaging the quantity for time increments $+t$ and $-t$, and we use the symbol $\mathcal{L}_{xx}(\Delta z, z', t)$ with three arguments to represent the Lagrangian correlation of b_x between points on two field lines connected to the origin, where one point is at parallel distance z' and the other is at a parallel distance increased by Δz and for a time incremented by $\pm t$ (averaging over the two cases). Because of the special role played by the origin in space, where the two field lines are at the same point, this correlation also depends on the parallel distance z' from the origin.

It is useful to define the perpendicular displacement $\Delta\boldsymbol{x}_\perp \equiv \boldsymbol{x}''_{\perp t} - \boldsymbol{x}'_{\perp t}$ and the time-differenced displacement $\boldsymbol{X}' \equiv \boldsymbol{x}'_{\perp t} - \boldsymbol{x}'_{\perp 0}$ and then write $\boldsymbol{x}''_{\perp t} - \boldsymbol{x}'_{\perp 0} = \Delta\boldsymbol{x}_\perp + \boldsymbol{X}'$, as illustrated in Figure 1.

From Equation (4), we find that

$$\Big\langle X^2(z, t)\Big\rangle = \frac{4}{B_0^2}\int_0^z \int_0^{z-z'} \Big[\mathcal{L}_{xx}(\Delta z) - \mathcal{L}_{xx}(\Delta z, z', t)\Big]d\Delta z dz', \quad (8)$$

where $\mathcal{L}_{xx}(\Delta z)$ as defined by Equation (3) is indeed the limit as $t \to 0$ (for any z') of $\mathcal{L}_{xx}(\Delta z, z', t)$ as defined by Equation (7), so the difference between them is small for low t. In fact, $\mathcal{L}_{xx}(\Delta z)$ is also the limit of $\mathcal{L}_{xx}(\Delta z, z', t)$ as $z' \to 0$ for any t. Note that typically $\mathcal{L}_{xx} \to 0$ as $\Delta z \to \infty$ (even at $t = 0$) and as $t \to \infty$. For any turbulence with a dependence on (x,y) (i.e., that is not slab turbulence), the random walk decorrelates the Lagrangian correlation and $\mathcal{L}_{xx} \to 0$ when $z' \to \infty$ as well.

At this point we invoke the first key assumption of this derivation, Corrsin's independence hypothesis (Corrsin 1959), which has been used (e.g., by Matthaeus et al. 1995) to approximate the Lagrangian correlation $\mathcal{L}_{xx}(\Delta z)$ in terms of $R_{xx}(\Delta\boldsymbol{x}_\perp, \Delta z, t = 0) \equiv \langle b_x(0, 0, 0)b_x(\Delta\boldsymbol{x}_\perp, \Delta z, 0)\rangle$. This involves averaging over the conditional probability $P(\Delta\boldsymbol{x}_\perp|\Delta z)$ of finding a displacement $\Delta\boldsymbol{x}_\perp$ after a distance Δz:

$$\mathcal{L}_{xx}(\Delta z) = \int R_{xx}\big(\Delta\boldsymbol{x}_\perp, \Delta z, 0\big)P\big(\Delta\boldsymbol{x}_\perp\big|\Delta z\big)d\Delta\boldsymbol{x}_\perp. \quad (9)$$

Here we also approximate $\mathcal{L}_{xx}(\Delta z, z', t)$ by averaging over the probability distributions of both $\Delta\boldsymbol{x}_\perp$ and $\boldsymbol{X}'$:[4]

$$\mathcal{L}_{xx}(\Delta z, z', t) = \int\int \Big[R_{xx}\big(\Delta\boldsymbol{x}_\perp + \boldsymbol{X}', \Delta z, t\big) \times P\big(\boldsymbol{X}'\big|z', t\big)\Big]_\pm P\big(\Delta\boldsymbol{x}_\perp\big|\Delta z\big)d\Delta\boldsymbol{x}_\perp d\boldsymbol{X}'. \quad (10)$$

It is useful to express an Eulerian correlation function such as $R_{xx}(\Delta\boldsymbol{x}_\perp, \Delta z, t)$ in terms of its spatial Fourier transform, the power spectrum $S_{xx}(\boldsymbol{k}, t)$. Following Bieber et al. (1994), we introduce a function $\Gamma(\boldsymbol{k}, t)$ to express the dynamical correlation:

$$\begin{aligned} S_{xx}(\boldsymbol{k}, t) &= S_{xx}(\boldsymbol{k}, 0)\Gamma(\boldsymbol{k}, t) \\ S_{yy}(\boldsymbol{k}, t) &= S_{yy}(\boldsymbol{k}, 0)\Gamma(\boldsymbol{k}, t), \end{aligned} \quad (11)$$

where we use the same function $\Gamma(\boldsymbol{k}, t)$ in both equations, and for brevity we will use $S_{xx}(\boldsymbol{k})$ to mean $S_{xx}(\boldsymbol{k}, 0)$, the power spectrum of the purely spatial Eulerian correlation function, and $S_{yy}(\boldsymbol{k})$ to mean $S_{yy}(\boldsymbol{k}, 0)$. By construction, $\Gamma(\boldsymbol{k}, t = 0) = 1$ for all $\boldsymbol{k}$, and for $t > 0$, $\Gamma(\boldsymbol{k}, t) = 1$ would indicate that there is no dynamical decorrelation. We also consider that the distribution of $\boldsymbol{X}'$ satisfies $P(\boldsymbol{X}'|z', -t) = P(\boldsymbol{X}'|z', t)$, by the statistical stationarity of the displacement distribution. Then

[4] The reason why we chose the ordering $z' \leqslant z''$ is so that $P(\boldsymbol{X}')$, for distance z', and $P(\Delta\boldsymbol{x}_\perp)$, for the displacement of a field line from z' to z'', can be considered causally independent and axisymmetric, i.e., that the displacement from z' to z'' is a Markov process that is uncorrelated with displacements up to z'. If we allowed the reverse ordering, $z' > z''$, in that case $P(\Delta\boldsymbol{x}_\perp)$ would be biased to the $-\boldsymbol{X}'$ direction, because on average $\boldsymbol{x}_{\perp 2}(z'')$ must be closer to the origin than $\boldsymbol{x}_{\perp 2}(z')$, and the latter is correlated with $\boldsymbol{X}'$. This subtlety was not recognized in the analogous field line separation calculation by Ruffolo et al. (2004). When imposing the ordering $z' \leqslant z''$, their results change slightly. For example, the bracketed term in their Equation (54) becomes $[g - g']$, i.e., the third term disappears and the second term is doubled. The qualitative conclusions and types of behavior reported by Ruffolo et al. (2004) remain unchanged.

Equation (10) becomes

$$\begin{aligned}\mathcal{L}_{xx}(\Delta z, z', t) &= \int\int\int\int S_{xx}(\boldsymbol{k})\Gamma_{\pm}(\boldsymbol{k}, t)\\ &\quad\times e^{i\boldsymbol{k}_\perp\cdot(\Delta\boldsymbol{x}_\perp+\boldsymbol{X}')+ik_z\Delta z}\\ &\quad\times P(\Delta\boldsymbol{x}_\perp|\Delta z)P(\boldsymbol{X}'|z', t)d\Delta\boldsymbol{x}_\perp d\boldsymbol{X}' d\boldsymbol{k}_\perp dk_z\\ &= \int\int S_{xx}(\boldsymbol{k})\Gamma_{\pm}(\boldsymbol{k}, t)e^{ik_z\Delta z}\\ &\quad\times\left[\int e^{i\boldsymbol{k}_\perp\cdot\Delta\boldsymbol{x}_\perp}P(\Delta\boldsymbol{x}_\perp|\Delta z)d\Delta\boldsymbol{x}_\perp\right]\\ &\quad\times\left[\int e^{i\boldsymbol{k}_\perp\cdot\boldsymbol{X}'}P(\boldsymbol{X}'|z', t)d\boldsymbol{X}'\right]d\boldsymbol{k}_\perp dk_z,\end{aligned} \tag{12}$$

where $\boldsymbol{k}_\perp \equiv (k_x, k_y)$ and $\Gamma_{\pm}(\boldsymbol{k}, t) \equiv [\Gamma(\boldsymbol{k}, t) + \Gamma(\boldsymbol{k}, -t)]/2$. Note that $S_{xx}(\boldsymbol{k})$ as used here follows a different Fourier transform convention than $P_{xx}(\boldsymbol{k})$ as used in some of our previous work; the physical results do not depend on the convention used. Note also that if there is more than one component of turbulence, as in the 2D+slab model, then $S_{xx}(\boldsymbol{k})$ is replaced by the sum of power spectra for each turbulence component, and the above integral is replaced by a sum of such integrals with $S^{(i)}_{xx}(\boldsymbol{k})\Gamma^{(i)}_{\pm}(\boldsymbol{k}, t)$ for each component i.

To evaluate the bracketed integrals, we use a second key assumption that the above probability distributions are Gaussian and independent for displacements in the x- and y-directions. We use σ_i^2 to denote the variance of the Gaussian distribution in quantity i. In this work we use equal variance in x and y, $\sigma_x^2(\Delta z) = \sigma_y^2(\Delta z)$, for the case of axisymmetric fluctuations. Then we obtain

$$\int e^{i\boldsymbol{k}_\perp\cdot\Delta\boldsymbol{x}_\perp}P(\Delta\boldsymbol{x}_\perp|\Delta z)d\Delta\boldsymbol{x}_\perp = e^{-k_\perp^2\sigma_x^2(\Delta z)/2}. \tag{13}$$

However, the variances of time-differenced displacements $\sigma_X^2(z', t)$ and $\sigma_Y^2(z', t)$ are not necessarily equal (e.g., when a preferred direction due to a mean flow breaks the symmetry) and we have

$$\int e^{i\boldsymbol{k}_\perp\cdot\boldsymbol{X}'}P(\boldsymbol{X}'|z', t)d\boldsymbol{X}' = e^{-k_x^2\sigma_X^2(z',t)/2}e^{-k_y^2\sigma_Y^2(z',t)/2}. \tag{14}$$

Now Equation (13) reduces to

$$\begin{aligned}\mathcal{L}_{xx}(\Delta z, z', t) &= \int\int S_{xx}(\boldsymbol{k})\Gamma_{\pm}(\boldsymbol{k}, t)e^{ik_z\Delta z}e^{-k_\perp^2\sigma_x^2(\Delta z)/2}\\ &\quad\times e^{-k_x^2\sigma_X^2(z',t)/2}e^{-k_y^2\sigma_Y^2(z',t)/2}d\boldsymbol{k}_\perp dk_z,\end{aligned} \tag{15}$$

where the functions $\sigma_x^2(\Delta z)$, $\sigma_X^2(z', t)$, and $\sigma_Y^2(z', t)$ need to be specified for closure of the problem. We can recover an expression for $\mathcal{L}_{xx}(\Delta z)$ along the same field line by taking $t \to 0$ and $\sigma_X^2,\ \sigma_Y^2 \to 0$ so that the distribution of $\boldsymbol{X}'$ is concentrated at zero:

$$\mathcal{L}_{xx}(\Delta z) = \int\int S_{xx}(\boldsymbol{k})e^{ik_z\Delta z}e^{-k_\perp^2\sigma_x^2(\Delta z)/2}d\boldsymbol{k}_\perp dk_z. \tag{16}$$

Substituting Equations (15) and (16) into Equation (8), we now find the mean-squared time-differenced FLRW to give

$$\begin{aligned}\left\langle X^2(z, t)\right\rangle &= \frac{4}{B_0^2}\int_0^z\int_0^{z-z'}\int\int S_{xx}(\boldsymbol{k})e^{ik_z\Delta z}e^{-k_\perp^2\sigma_x^2(\Delta z)/2}\\ &\quad\times\left[1 - \Gamma_{\pm}(\boldsymbol{k}, t)e^{-k_x^2\sigma_X^2(z',t)/2}e^{-k_y^2\sigma_Y^2(z',t)/2}\right]\\ &\quad\times d\boldsymbol{k}_\perp dk_z d\Delta z dz'\end{aligned} \tag{17}$$

and a similar expression for $\langle Y^2(z, t)\rangle$ in which S_{xx} is replaced by S_{yy}. We can also express the mean-squared FLRW as

$$\begin{aligned}\left\langle x^2(z)\right\rangle = \left\langle y^2(z)\right\rangle &= \frac{2}{B_0^2}\int_0^z\int_0^{z-z'}\int\int\\ &\quad\times S_{xx}(\boldsymbol{k})e^{ik_z\Delta z}e^{-k_\perp^2\sigma_x^2(\Delta z)/2}d\boldsymbol{k}_\perp dk_z d\Delta z dz'.\end{aligned} \tag{18}$$

Finally, we note that for most types of turbulence, we expect the FLRW and time-differenced FLRW to tend to Markovian random walks after sufficient parallel distance z, so that the random walk becomes diffusive with $\langle x^2\rangle \propto z$ and $\langle X^2\rangle \propto z$. It is therefore useful to define running diffusion coefficients such that

$$D_X \equiv \frac{1}{2}\frac{d\left\langle X^2\right\rangle}{dz} \qquad D_x \equiv \frac{1}{2}\frac{d\left\langle x^2\right\rangle}{dz}. \tag{19}$$

Transforming from Δz back to $z'' = z' + \Delta z$, switching the limits of integration of z' and z'', and taking the derivative with respect to z, the limit of integration, we obtain

$$\begin{aligned}D_X(z, t) &= \frac{2}{B_0^2}\int_0^z\int\int S_{xx}(\boldsymbol{k})e^{ik_z(z-z')}e^{-k_\perp^2\sigma_x^2(z-z')/2}\\ &\quad\times\left[1 - \Gamma_{\pm}(\boldsymbol{k}, t)e^{-k_x^2\sigma_X^2(z',t)/2}e^{-k_y^2\sigma_Y^2(z',t)/2}\right]\\ &\quad\times d\boldsymbol{k}_\perp dk_z dz'\end{aligned} \tag{20}$$

$$\begin{aligned}D_x(z) &= \frac{1}{B_0^2}\int_0^z\int\int S_{xx}(\boldsymbol{k})e^{ik_z\Delta z}\\ &\quad\times e^{-k_\perp^2\sigma_x^2(\Delta z)/2}d\boldsymbol{k}_\perp dk_z d\Delta z,\end{aligned} \tag{21}$$

where we have simplified the final integral by substituting $\Delta z = z - z'$. Note that Equations (20) and (21) are consistent with Equation (5) at large t if $\Gamma \to 0$ in that limit.

2.4. Dynamical Correlation

The dynamical correlation $\Gamma(\boldsymbol{k}, t)$ can result from a variety of factors, as discussed previously in the literature (Bieber et al. 1994; Matthaeus & Bieber 1999; Zhou et al. 2004; Shalchi et al. 2006):

1. *Convection.* If there is an overall wind flow $\boldsymbol{V}$, then the turbulence will be convected past the region of interest. This effectively shifts the correlation pattern by $\boldsymbol{V}t$, which in wavenumber space corresponds to multiplication of the dynamic correlation by $e^{i\boldsymbol{k}\cdot\boldsymbol{V}t}$. Once this factor is included, all other dynamical effects can be estimated in the rest frame of the bulk plasma.
2. *Wave propagation.* For a component of turbulence that corresponds to propagating waves, such as Alfvén waves, the contribution of wavenumber $\boldsymbol{k}$ propagates at one or more possible frequencies $\omega_j(\boldsymbol{k})$. The dynamical

correlation due to wave propagation is $\sum_j f_j(\boldsymbol{k}) e^{i\omega_j(\boldsymbol{k})t}$, where $f_j(\boldsymbol{k})$ is the fraction of the power spectrum that is associated with each ω_j. For the case of shear Alfvén waves, there are two modes $\omega = \pm k_z v_A$, where v_A is the Alfvén speed. If these modes have equal energy, the dynamical correlation due to wave propagation is $\cos(k_z v_A t)$. For the case of a non-propagating mode, $\omega_j = 0$ and $e^{i\omega_j t} = 1$, in which case wave propagation has no effect on $\Gamma(\boldsymbol{k}, t)$.

3. *Local nonlinear distortion.* This accounts for evolution of the turbulence according to nonlinear processes, such as vortex stretching. Various functional forms have been proposed, and one convenient choice is to multiply the dynamical correlation by $e^{-|t|/\tau_{\rm NL}(\boldsymbol{k})}$ (Zhou et al. 2004). In the next section, we will propose a specific formula for $\tau_{\rm NL}(\boldsymbol{k})$ in noisy RMHD turbulence.
4. *Random sweeping.* This is the contribution of random sweeping of spatially varying structures past the region of interest (Chen & Kraichnan 1989; Matthaeus & Bieber 1999). In a turbulent plasma, smaller-scale structures at $\boldsymbol{k}$ in the inertial range are decorrelated due to sweeping by larger-scale structures with speed $\boldsymbol{v}$. The sweeping frequency is $\omega = \boldsymbol{k} \cdot \boldsymbol{v}$, and when we consider only transverse fluctuations with $\boldsymbol{b} \perp \boldsymbol{B}_0$ and $\boldsymbol{v} \perp \boldsymbol{B}_0$, this sweeping effect depends on the perpendicular magnitude of the wave vector, $k_\perp$. We use a dynamical correlation of $e^{-k_\perp^2 u_\perp^2 t^2/2}$ if $k_\perp \lambda_{c2} > 1$, for the inertial range, where $u_\perp$ is the (transverse) velocity amplitude of the quasi-2D portion of the turbulence, e.g., as defined by Oughton et al. (2006), and λ_{c2} is the total correlation length of the quasi-2D fluctuations, as defined by Matthaeus et al. (2007). Otherwise we use 1 to imply no sweeping decorrelation for component wave vectors in the energy-containing range.

Here we consider that each of these effects may contribute to dynamical decorrelation, i.e., a value of Γ less than 1, and therefore we multiply these effects to obtain an overall expression for Γ:

$$\Gamma(\boldsymbol{k}, t) = e^{i\boldsymbol{k}\cdot\boldsymbol{V}t}\left(\sum_j f_j(\boldsymbol{k}) e^{i\omega_j(\boldsymbol{k})t}\right) e^{-|t|/\tau_{\rm NL}(\boldsymbol{k})} \times e^{-H(k_\perp\lambda_{c2}-1)k_\perp^2 u_\perp^2 t^2/2}, \quad (22)$$

where H is the Heaviside step function that is 1 for a positive argument and 0 otherwise. Various terms can be nonaxisymmetric in k_x and k_y, and in particular the $e^{i\boldsymbol{k}\cdot\boldsymbol{V}t}$ term is nonaxisymmetric for a wind that is not completely along $\boldsymbol{B}_0$, such as the solar wind. In Equation (17) and the analogous equation for $\langle Y^2(z, t)\rangle$, $S_{xx}(\boldsymbol{k})$ and $S_{yy}(\boldsymbol{k})$ have different functional forms (due to the solenoidal property of $\boldsymbol{b}$), so a nonaxisymmetric $\Gamma(\boldsymbol{k}, t)$ can lead to different expressions for $\langle X^2\rangle$ and $\langle Y^2\rangle$.

In the past some studies have chosen to include some effects and not others; for example, Bieber et al. (1994) chose to invoke either sweeping or a type of nonlinear distortion. We note that the intention of the sweeping model is to *reduce* Γ (for stronger decorrelation) due to sweeping of small-scale structures by larger-scale structures. However, at low t the sweeping term has very little effect (with zero slope at $t = 0$) and using this term alone results in *higher* Γ (weaker decorrelation) in comparison with the nonlinear distortion term. We therefore consider that when it is applicable, the sweeping term should multiply other relevant terms rather than replacing them, and then the sweeping has little effect at low t but reduces Γ at high t. By extension of this logic we have multiplied all the relevant terms together to obtain Γ, following Zhou et al. (2004).

The equations for the time-differenced FLRW use $\Gamma_\pm(\boldsymbol{k}, t) \equiv [\Gamma(\boldsymbol{k}, t) + \Gamma(\boldsymbol{k}, -t)]/2$, which is given by

$$\begin{aligned}\Gamma_\pm(\boldsymbol{k}, t) &= \frac{1}{2}\left(\sum_j f_j(\boldsymbol{k})\left\{e^{i[\boldsymbol{k}\cdot\boldsymbol{V}+\omega_j(\boldsymbol{k})]t} + e^{-i[\boldsymbol{k}\cdot\boldsymbol{V}+\omega_j(\boldsymbol{k})]t}\right\}\right) \\ &\quad\times e^{-|t|/\tau_{\rm NL}(\boldsymbol{k})} e^{-H(k_\perp\lambda_{c2}-1)k_\perp^2 u_\perp^2 t^2/2} \\ &= \left(\sum_j f_j(\boldsymbol{k})\cos\left\{\left[\boldsymbol{k}\cdot\boldsymbol{V} + \omega_j(\boldsymbol{k})\right]t\right\}\right) \\ &\quad\times e^{-|t|/\tau_{\rm NL}(\boldsymbol{k})} e^{-H(k_\perp\lambda_{c2}-1)k_\perp^2 u_\perp^2 t^2/2}.\end{aligned} \quad (23)$$

Note that it is possible for $\Gamma_\pm(\boldsymbol{k}, t)$ to be negative, corresponding to a dynamical anticorrelation, due to the effects of the wind and waves.

2.5. Short-distance Behavior

A turbulent power spectrum $S_{xx}(\boldsymbol{k})$ should be mostly concentrated over a finite wavenumber range $|k_z| \lesssim k_{0z} = 1/\ell_z$ for a parallel coherence length ℓ_z and $k_\perp \lesssim k_{0\perp} = 1/\ell_\perp$ for a perpendicular coherence length $\ell_\perp$. We consider the short-distance régime to be the range of z sufficiently small that $k_{0z}z$, $k_{0\perp}\sigma_x$, $k_{0\perp}\sigma_X$, and $k_{0\perp}\sigma_Y$ are all $\ll 1$. Given that the integral of the power spectrum is $R_{xx}(0, 0, 0) = \langle b_x^2\rangle$,

$$\left\langle b_x^2\right\rangle = \int\int S_{xx}(\boldsymbol{k}) d\boldsymbol{k}_\perp dk_z, \quad (24)$$

then from Equations (17) and (18), it is straightforward to show that in the short-distance régime,

$$\left\langle x^2(z)\right\rangle = \frac{\left\langle b_x^2\right\rangle}{B_0^2} z^2, \quad (25)$$

$$\left\langle X^2(z, t)\right\rangle = 2\left[1 - \bar{\Gamma}_x(t)\right]\left\langle x^2(z)\right\rangle = 2\left[1 - \bar{\Gamma}_x(t)\right]\frac{\left\langle b_x^2\right\rangle}{B_0^2} z^2, \quad (26)$$

where $\bar{\Gamma}_x(t)$ is the $\boldsymbol{k}$-average of $\Gamma_\pm(\boldsymbol{k}, t)$ weighted by the power spectrum $S_{xx}(\boldsymbol{k})$:

$$\bar{\Gamma}_x(t) \equiv \frac{\int S_{xx}(\boldsymbol{k})\Gamma_\pm(\boldsymbol{k}, t) d\boldsymbol{k}}{\int S_{xx}(\boldsymbol{k}) d\boldsymbol{k}} = \frac{R_{xx}(0, t)}{R_{xx}(0, 0)}. \quad (27)$$

Then $\langle Y^2(z, t)\rangle$ is given by the same expression with $\bar{\Gamma}_x$ replaced by $\bar{\Gamma}_y$, which is defined similarly in terms of $S_{yy}(\boldsymbol{k})$. Note that $\bar{\Gamma}_x$ in Equation (28) is just the familiar (normalized) Eulerian time correlation function, i.e., the single-point, two-time correlation.

We refer to $\bar{\Gamma}_i(t)$ as a mean dynamical correlation. It is possible for this quantity to be negative in certain ranges

of t, corresponding to a dynamical anticorrelation, in which case $\langle X^2(z, t)\rangle > 2\langle x^2(z)\rangle$, and the time-differenced mean-squared displacement at small z is found to be temporarily *greater* than that between two uncorrelated field lines.

Equation (26) can be rearranged in a physically revealing form as

$$\left\langle X^2(z, t)\right\rangle = \frac{\left\langle \left[b_x(0,\ 0) - b_x(0, t)\right]^2\right\rangle}{B_0^2} z^2. \tag{28}$$

In other words, at short distance z, the variance of the time-differenced displacement at any time t is simply the 2nd-order temporal structure function normalized to B_0^2 and multiplied by z^2. If we have a model of the Eulerian time correlation function, that directly implies a model for $\langle X^2(z, t)\rangle$ at low z. In this form we can confirm that as $t \to 0$ we have $\langle X^2(z, t)\rangle \to 0$, and as $t \to \infty$ we have $\langle X^2(z, t)\rangle \to 2(\langle b_x^2\rangle/B_0^2)z^2$, which is twice the mean squared field line displacement in this ballistic régime.

Note that $\bar{\Gamma}_i(t)$ is directly related to single-point observations (e.g., at a single spacecraft). It expresses the time-lagged correlation function of a magnetic field component divided by the correlation at zero time lag. If we set the wind speed $\boldsymbol{V}$ to zero, then $\bar{\Gamma}_i(t)$ expresses the normalized Eulerian correlation function in the zero-momentum frame of the plasma. Recently both types of correlation functions have been measured for fast and slow solar wind outside Earth's magnetosphere using data from multiple spacecraft (Weygand et al. 2013).

Equation (26) expresses that in the short-distance régime, there is free-streaming (ballistic) behavior for both the field line displacement ($x_{\rm rms} \propto z$) and the time-differenced displacement ($X_{\rm rms}$, $Y_{\rm rms} \propto z$) as a function of the parallel distance z, i.e., the field lines are typically straight lines over such a short distance.

2.6. Closure by Random Ballistic Decorrelation

To obtain a result that is valid for all distances we must analyze Equations (20) and (21) in greater detail. Returning to Equation (17) for the time-differenced FLRW as a function of distance z and time separation t, there is a closure issue: how to specify $\sigma_x^2(\Delta z)$, $\sigma_X^2(z', t)$, and $\sigma_Y^2(z', t)$. Three closure models have been used in the FLRW literature: self-closure to derive a second-order ODE, diffusive decorrelation (DD), and random ballistic decorrelation (RBD). These led to three versions of Corrsin-based theories of the FLRW, which had similar accuracy in comparison with computer simulations for 2D+slab magnetic fluctuations (Ghilea et al. 2011; Snodin et al. 2013a). For the FLRW in a model of "noisy" RMHD, the RBD version was closest to the simulation results at moderately high Kubo number (Snodin et al. 2013b). For isotropic turbulence with zero mean field, the RBD closure matches some aspects of the simulated FLRW better than other versions (Sonsrettee et al. 2015). For the perpendicular diffusion of particles, nonlinear guiding center theory (Matthaeus et al. 2003) as modified to use RBD and a backtracking correction (Ruffolo et al. 2012) exhibited greatly improved agreement with direct simulation results. In some cases, use of the RBD closure leads to simpler theoretical expressions (e.g., Ruffolo et al. 2012).

For the time-differenced FLRW, we find that the self-closure and DD closure have deficiencies, as described in appendix. Therefore, for the remainder of this work we will use the RBD closure. This closure provides explicit integral equations that are convenient for numerical evaluation.

In the RBD closure, we use the short-distance (ballistic) behavior expressed by Equations (25) and (26) to specify

$$\begin{aligned}
\sigma_x^2(\Delta z) &= \frac{\left\langle b_x^2\right\rangle}{B_0^2}\Delta z^2 \\
\sigma_X^2(z', t) &= 2\left[1 - \bar{\Gamma}_x(t)\right]\frac{\left\langle b_x^2\right\rangle}{B_0^2} z'^2 \\
\sigma_Y^2(z', t) &= 2\left[1 - \bar{\Gamma}_y(t)\right]\frac{\left\langle b_y^2\right\rangle}{B_0^2} z'^2,
\end{aligned} \tag{29}$$

and we continue to use the assumption that the fluctuations are axisymmetric with $\langle b_x^2\rangle = \langle b_y^2\rangle$. We stress that the use of these formulas does not preclude other types of intermediate behavior of $\langle x^2\rangle$ and $\langle X^2\rangle$. Substituting these into Equation (17), we obtain

$$\begin{aligned}
\left\langle X^2(z, t)\right\rangle = \frac{4}{B_0^2}\int_0^z \int_0^{z-z'} \int\int S_{xx}(\boldsymbol{k}) e^{ik_z\Delta z} \\
\times e^{-k_\perp^2\left(\left\langle b_x^2\right\rangle/B_0^2\right)\Delta z^2/2} \\
\times \Big[1 - \Gamma_\pm(\boldsymbol{k}, t) \\
\times e^{-\left\{k_x^2\left[1-\bar{\Gamma}_x(t)\right]+k_y^2\left[1-\bar{\Gamma}_y(t)\right]\right\}\left(\left\langle b_x^2\right\rangle/B_0^2\right)z'^2}\Big] \\
\times d\boldsymbol{k}_\perp dk_z d\Delta z dz'.
\end{aligned} \tag{30}$$

This can be converted to a formula for $\langle Y^2(z, t)\rangle$ by the substitution $S_{xx}(\boldsymbol{k}) \to S_{yy}(\boldsymbol{k})$. Now we have a general expression for the time-differenced FLRW that depends only on the magnetic fluctuation power spectrum and its dynamical correlation.

3. CALCULATIONS FOR NOISY REDUCED MAGNETOHYDRODYNAMIC TURBULENCE

To illustrate the concepts developed in this work for a specific form of turbulent magnetic fluctuations, we consider the noisy RMHD model. RMHD itself involves a set of MHD equations for the limit of transverse fluctuations, a basic feature of MHD in a strong mean field that develops wavenumber anisotropy (Strauss 1976; Kadomtsev & Pogutse 1979; Montgomery 1982; Zank & Matthaeus 1992; Kinney & McWilliams 1998), which occurs most readily in models that are weakly compressive (Matthaeus et al. 1996). The model is relevant to astrophysical plasmas with a strong large-scale field, e.g., to explain heating in solar coronal loops (Dmitruk et al. 1998) and the open field line corona (Oughton et al. 2001; Perez & Chandran 2013), and interchange reconnection and the origin of the slow solar wind (Rappazzo et al. 2012).

Noisy RMHD is a synthetic model in which the power spectrum is specified by an analytic function in order to approximate the form of transverse RMHD fluctuations,

as generalized to allow a general Kubo number, $R = (b/B_0)(\ell_\parallel/\ell_\perp)$, where b is the rms magnetic fluctuation, and $\ell_\parallel$ and $\ell_\perp$ are correlation scales parallel and perpendicular to the mean field, respectively. As before, the total magnetic field is $\boldsymbol{B} = B_0\hat{\boldsymbol{z}} + \boldsymbol{b}(\boldsymbol{x})$, and now the statistically homogeneous fluctuating field is given by

$$\boldsymbol{b}(x, y, z) = \nabla_\perp \times \left[a(x, y, z)\hat{\boldsymbol{z}}\right], \tag{31}$$

where the subscript "$\perp$" indicates a projection perpendicular to the mean field in which only x- and y-components are included. We refer to the scalar a as the potential function. In terms of wave vectors $\boldsymbol{k}$, we can write

$$\boldsymbol{b}(\boldsymbol{k}) = i\boldsymbol{k}_\perp \times \left[a(\boldsymbol{k})\hat{\boldsymbol{z}}\right], \tag{32}$$

and we specify the potential function in $\boldsymbol{k}$-space by

$$a(\boldsymbol{k}) \propto \begin{cases} a^{2\mathrm{D}}\left(k_x, k_y\right)e^{i\varphi(\boldsymbol{k})} & \text{for } \left|k_z\right| \leqslant K \\ 0 & \text{for } \left|k_z\right| > K, \end{cases} \tag{33}$$

where $\varphi(\boldsymbol{k})$ is a random phase. In terms of the power spectra, this model gives

$$S_{xx}(\boldsymbol{k}) = \begin{cases} k_y^2 A\left(k_x, k_y\right)\big/(2K) & \text{for } \left|k_z\right| \leqslant K \\ 0 & \text{for } \left|k_z\right| > K \end{cases}$$
$$S_{yy}(\boldsymbol{k}) = \begin{cases} k_x^2 A\left(k_x, k_y\right)\big/(2K) & \text{for } \left|k_z\right| \leqslant K \\ 0 & \text{for } \left|k_z\right| > K, \end{cases} \tag{34}$$

where A is the 2D power spectrum of $a^{2\mathrm{D}}$. This "boxcar" dependence on k_z has previously been used to characterize the results of RMHD simulations Oughton et al. (2004). For this spectrum, the parallel correlation length is $\ell_\parallel = \pi/(2K)$. Then the FLRW is characterized by the Kubo number (Pommois et al. 2001),

$$R = \frac{b}{B_0}\frac{\ell_\parallel}{\ell_\perp} = \frac{b}{B_0}\frac{\pi}{2K\lambda_{c2}}. \tag{35}$$

This macroscopic definition of the Kubo number describes the scaling of field line diffusion and does not directly express the Kolmogorov entropy or other microscopic properties. For this model, previous studies have examined the FLRW by analytic theory (Ruffolo & Matthaeus 2013) and computer simulations (Snodin et al. 2013b), as well as the perpendicular diffusion of particles (Shalchi & Hussein 2014).

Now let us specify the physical parameters needed to derive the dynamical correlation $\Gamma_\pm(\boldsymbol{k}, t)$. Since this model could be applied to plasma in a solar coronal loop, where there is often little or no bulk flow, we set $V = 0$. This is a substantial simplification; now Equation (23) is naturally axisymmetric about $\boldsymbol{B}_0$, and given our assumption of axisymmetric magnetic fluctuations, we have $\langle X^2\rangle = \langle Y^2\rangle$ and $\bar{\Gamma}_x(t) = \bar{\Gamma}_y(t)$, so we can suppress the subscripts in this case. Continuing to specify the parameters for Equation (23), we consider $\omega_j(\boldsymbol{k})$ to correspond to Alfvén waves that propagate along $\hat{\boldsymbol{z}}$ with speed $\pm v_A$. Then the wave term in Equation (23) becomes $\cos(v_A k_z t)$.

To specify the nonlinear time, we use a form similar to that used by Shalchi et al. (2006), with a constant decorrelation rate for the energy-containing range of turbulence (i.e., for wavenumbers below the outer scale) corresponding to the outer scale eddy turnover time, and a $\boldsymbol{k}$-dependent decorrelation rate for the inertial range according to the local eddy turnover time in Kolmogorov theory:

$$\frac{1}{\tau_{\mathrm{NL}}} = \begin{cases} 1/\tau_0 & k_\perp\lambda_{c2} \leqslant 1 \\ 1/\tau\left(k_\perp\right) & k_\perp\lambda_{c2} > 1, \end{cases}$$
$$= \frac{u_\perp}{\lambda_{c2}}\begin{cases} 1 & k_\perp\lambda_{c2} \leqslant 1 \\ \left(k_\perp\lambda_{c2}\right)^{2/3} & k_\perp\lambda_{c2} > 1. \end{cases} \tag{36}$$

Now we can express the dynamical correlation from Equation (23) as

$$\Gamma_\pm(\boldsymbol{k}, t) = \cos\left(v_A k_z t\right)e^{-\left\{1+H\left(k_\perp\lambda_{c2}-1\right)\left[\left(k_\perp\lambda_{c2}\right)^{2/3}-1\right]\right\}|t|/\tau_0}$$
$$\times\, e^{-H\left(k_\perp\lambda_{c2}-1\right)k_\perp^2 u_\perp^2 t^2/2}, \tag{37}$$

where the three multiplicative terms on the right hand side are the wave term, nonlinear term, and sweeping term. For calculation it is convenient to use the dimensionless units $t' = t/\tau_0$, $x' = x/\lambda_{c2}$, $k_z' = k_z/K$, etc. Then the above equation can be simplified to read

$$\Gamma_\pm\left(\boldsymbol{k}', t'\right) = \cos\left(\frac{\pi}{2}\frac{k_z' t'}{R}\right)$$
$$\times\, e^{-\left\{1+H\left(k_\perp'-1\right)\left[k_\perp'^{2/3}-1\right]\right\}|t'|}e^{-H\left(k_\perp'-1\right)k_\perp'^2 t'^2/2}, \tag{38}$$

where we have used $u_\perp/v_A = b/B_0$ following Shalchi et al. (2006), which physically corresponds to an assumption of equipartition between magnetic and velocity fluctuations in the turbulence. Here only the wave term depends on the Kubo number.

To visualize the effects of these terms, we have calculated the Eulerian time decorrelation Equation (27) in terms of a noisy RMHD power spectrum. Following Ruffolo & Matthaeus (2013), we use the spectrum of Equation (34), where

$$A\left(k_\perp\right) \propto \frac{1}{\left[1 + \left(k_\perp\lambda_\perp\right)^2\right]^{7/3}}, \tag{39}$$

which is normalized to produce our choice for b. The above form for $A(k_\perp)$ has the properties that the omnidirectional 2D power spectrum at high $k_\perp$ is proportional to $k_\perp^{-5/3}$, representing Kolmogorov scaling in the perpendicular wave vectors in the inertial range (Ruffolo et al. 2004), and the low-$k_\perp$ behavior satisfies the requirements of strict homogeneity (Matthaeus et al. 2007). In practice, for all numerical demonstrations, as well as in nature, there is always a high wavenumber cutoff. From Equation (27), we have

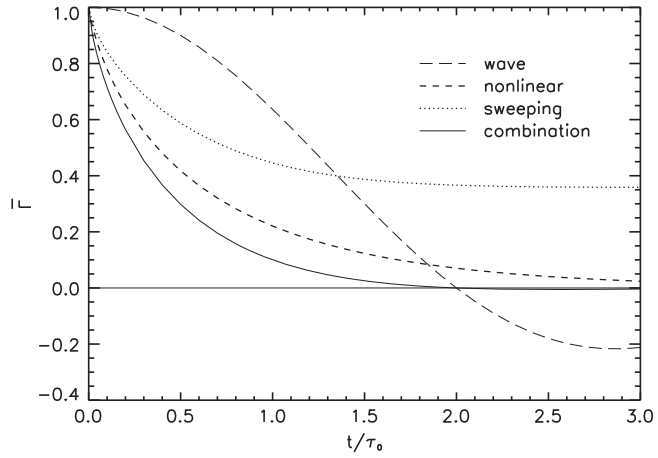

Figure 2. Mean dynamical correlation $\bar{\Gamma}$ as a function of time separation t for noisy RMHD turbulence with Kubo number $R = 1$, both for individual processes and for all processes in combination. We are working in the plasma rest frame (wind speed $V = 0$), so $\bar{\Gamma}(t)$ represents the normalized Eulerian correlation function. In this and other figures, t is expressed in units of τ_0, the outer scale eddy turnover time. Here the Alfvén wave term plays a special role by bringing $\bar{\Gamma}$ to zero at a finite time, which depends on R, while the nonlinear term causes an overall decrease that is independent of R in these units.

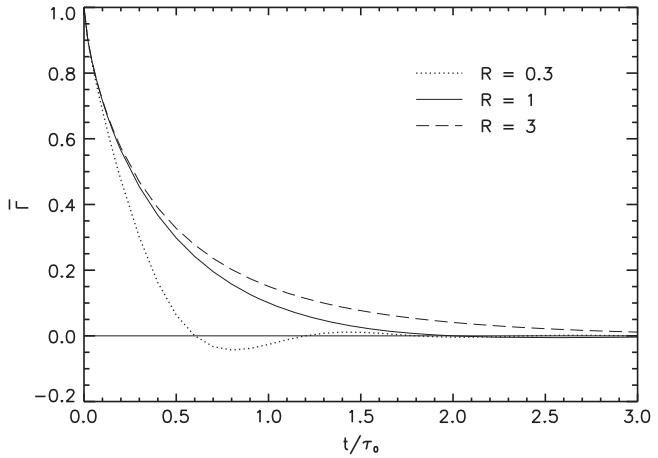

Figure 3. Mean dynamical correlation $\bar{\Gamma}$ as a function of time separation t for noisy RMHD turbulence at Kubo number $R = 0.3$, 1, and 3. The approach to zero is affected by the Alfvén wave term (see Figure 2), which for $R \lesssim 1$ leads to a reduced correlation time scale for lower R.

$$\bar{\Gamma}(t') \equiv \frac{\int S_{xx}(\boldsymbol{k}')\Gamma_{\pm}(\boldsymbol{k}', t')d\boldsymbol{k}'}{\int S_{xx}(\boldsymbol{k}')d\boldsymbol{k}'} = \frac{2R}{\pi t'}\sin\left(\frac{\pi t'}{2R}\right) \times \left(\int_0^\infty k_\perp'^3 A(k_\perp') e^{-\left\{1+H(k_\perp'-1)\left[k_\perp'^{2/3}-1\right]\right\}|t'|} \times e^{-H(k_\perp'-1)k_\perp'^2 t'^2/2} dk_\perp'\right) \Big/ \left(\int_0^\infty k_\perp'^3 A(k_\perp') dk_\perp'\right). \quad (40)$$

We have numerically evaluated $\bar{\Gamma}(t)$ from this equation using the Mathematica program (Wolfram Research, Inc.). Figure 2 shows $\bar{\Gamma}(t)$ when using individual terms in Equation (41), and when using all terms in combination. The Alfvén wave term plays a special role, bringing $\bar{\Gamma}(t)$ to zero at $t/\tau_0 = t' = 2R$. The nonlinear term causes an overall decline that is independent of R in these units. As a result, we see that at low Kubo number, $R < 1$, the duration of dynamical correlation is dominated by the wave term, whereas at $R \gtrsim 1$ it is dominated by the nonlinear term.

Figure 3 shows $\bar{\Gamma}$ versus t for all terms combined for $R = 0.3$, 1, and 3. It can be seen that at $R < 1$, there is a rapid decline and oscillation, with zero crossings at $t/\tau_0 = 2nR$ for integer n, due to the wave term. For $R \gtrsim 1$, the wave term has less effect, as the decline is dominated by the nonlinear term.

Given $\Gamma_{\pm}(\boldsymbol{k}, t)$ and $\bar{\Gamma}(t)$, we can proceed to evaluate the mean squared time-differenced displacement $\langle X^2(z, t)\rangle = \langle Y^2(z, t)\rangle$. We apply Equation (31) for the RMHD model, with axisymmetric dynamical decorrelation, and integrate over k_z from $-K$ to K to obtain

$$\left\langle X^2(z, t)\right\rangle = \frac{8\pi}{B_0^2}\int_0^z \int_0^{z-z'} \int_0^\infty k_\perp^3 A(k_\perp)\frac{\sin(K\Delta z)}{\Delta z} \times e^{-k_\perp^2\left(b^2/B_0^2\right)\Delta z^2/4} \times \left[1 - \cos(v_A K t)\right] \times e^{-\left\{1+H(k_\perp\lambda_{c2}-1)\left[\left(k_\perp^2\lambda_{c2}^2\right)^{2/3}-1\right]\right\}|t|/\tau_0} \times e^{-H(k_\perp\lambda_{c2}-1)k_\perp^2 u_\perp^2 t^2/2} e^{-k_\perp^2\left[1-\bar{\Gamma}(t)\right]\left(b^2/B_0^2\right)z'^2/2}\Big] \times dk_\perp d\Delta z dz'. \quad (41)$$

In terms of diffusion coefficients, in analogy to the derivations of Equations (21) and (22), for the time-differenced displacement we obtain

$$D_X = \frac{4\pi}{B_0^2}\int_0^z \int_0^\infty k_\perp^3 A(k_\perp)\frac{\sin[K(z-z')]}{z-z'} \times e^{-k_\perp^2\left(b^2/B_0^2\right)(z-z')^2/4} \times \Bigg[1 - \cos(v_A K t) e^{-\left\{1+H(k_\perp\lambda_{c2}-1)\left[\left(k_\perp^2\lambda_{c2}^2\right)^{2/3}-1\right]\right\}|t|/\tau_0} \times e^{-H(k_\perp\lambda_{c2}-1)k_\perp^2 u_\perp^2 t^2/2} e^{-k_\perp^2\left[1-\bar{\Gamma}(t)\right]\left(b^2/B_0^2\right)z'^2/2}\Bigg] dk_\perp dz', \quad (42)$$

and for the FLRW we obtain

$$D_x = \frac{2\pi}{B_0^2}\int_0^z \int_0^\infty k_\perp^3 A(k_\perp)\frac{\sin(K\Delta z)}{\Delta z} \times e^{-k_\perp^2\left(b^2/B_0^2\right)\Delta z^2/4} dk_\perp d\Delta z. \quad (43)$$

Figure 4 shows the diffusion coefficient D_X of the time-differenced displacement as a function of distance z along the mean magnetic field for noisy RMHD turbulence with various time displacements t for various Kubo numbers R. In the limit of large t or z, the two field lines for different

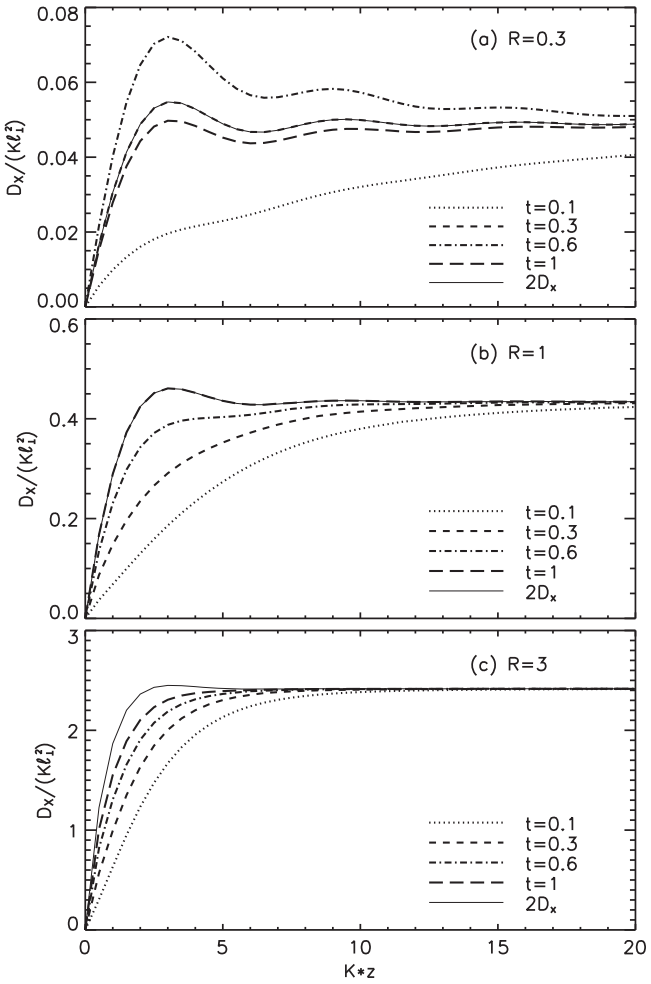

Figure 4. Diffusion coefficient D_X of the time-differenced displacement as a function of distance z along the mean magnetic field for noisy RMHD turbulence with various time displacements t (in units of τ_0), where the Kubo number is (a) $R = 0.3$, (b) $R = 1$, and (c) $R = 3$. In the limit of large t or z, the two field lines for different times (see Figure 1) undergo independent random walks, so $D_X \to 2D_x$, where D_x is the single field line diffusion coefficient, and we also plot $2D_x$ for comparison (thin solid lines). At finite t, D_X is lower (higher) than $2D_x$ for a positive (negative) dynamical correlation term. At low Kubo number (the quasilinear regime), D_X can oscillate in both t and z. This is demonstrated in panel (a) for $R = 0.3$, where at $t = 0.1$ we have low D_X because of the strong dynamical correlation, at $t = 0.3$ we have $D_X = 2D_x$ because the dynamical correlation term is zero, and at $t = 0.6$ we have $D_X > 2D_x$ because of the negative dynamical correlation term. The oscillations continue with decreasing amplitude at greater t. For large R, D_X monotonically tends to $2D_x$ with increasing t and converges to $2D_x$ more rapidly as a function of z.

times (see Figure 1) undergo independent random walks, so $D_X \to 2D_x$, where D_x is the single field line diffusion coefficient. At finite t, D_X is lower (higher) than $2D_x$ for a positive (negative) dynamical correlation term. At low Kubo number (the quasilinear regime), D_x can oscillate in both t and z due to the Alfvén wave term in the dynamical correlation. This is demonstrated in panel (a) for $R = 0.3$, where at $t = 0.1$ we have low D_x because of the strong dynamical correlation, at $t = 0.3$ we have $D_X = 2D_x$ because the dynamical correlation term is zero, and at $t = 0.6$ we have $D_X > 2D_x$ because of the negative dynamical correlation term. The oscillations continue with decreasing amplitude at greater t. For larger Kubo number, D_X monotonically tends to $2D_x$ with increasing t, and it converges to $2D_x$ more rapidly as a function of z.

4. SUMMARY AND DISCUSSION

In this work, we have developed an analytic theory for the statistics of the displacement X between two field lines in dynamical transverse magnetic turbulence that connect from a given point at two different times, separated by t, after the field lines are traced for a distance z along the mean field, as illustrated in Figure 1. We note again that for all numerical demonstrations, as well as in nature, there is always a high wavenumber cutoff in the power spectrum, so we have $X \to 0$ as $t \to 0$ or $z \to 0$. It is also expected that for turbulent-like fluctuations at large t or z, $\langle X^2(z, t)\rangle \to 2\langle x^2(z)\rangle$, where $\langle x^2(z)\rangle$ is the mean squared FLRW displacement, for a single field line after a distance z. This is expected because at large t or large z the two field lines become independent of one another. For standard types of turbulence, the FLRW becomes diffusive at high z, with $\langle X^2\rangle \propto z$ and $\langle x^2\rangle \propto z$. Thus it is convenient to display the results in terms of running diffusion coefficients, $D_X \equiv (1/2)d\langle X^2\rangle/dz$ and $D_x \equiv (1/2)d\langle x^2\rangle/dz$.

As we have tried to emphasize in the above presentation, the problem of time-differenced field line separation beginning from a specified spatial position has several features in common with FLRW, and also with field line separation at a single time. It is reasonable to ask why we formulated the problem in this way, which has intentionally avoided the idea of magnetic field lines that pass through a single material element (e.g., a plasma element) which itself is subject to convection and other dynamical effects. The reason to avoid this is that individual magnetic field lines are difficult to follow in time for the general case in which non-ideal effects are present and magnetic reconnection may occur (see, e.g., Newcomb 1958). Here, by selecting the two field lines of interest in a different and well-defined way, without an attempt to follow a given field line in time, one may formulate a connectivity problem in an unambiguous way.

We have developed a nonperturbative analytic framework based on Corrsin's hypothesis, which calculates $\langle X^2(z, t)\rangle$ given the fluctuation power spectrum $S_{xx}(\boldsymbol{k})$ and the dynamical correlation $\Gamma(\boldsymbol{k}, t)$. We propose that the dynamical correlation combines effects of convection due to a bulk flow, wave propagation, local nonlinear distortion, and random sweeping. Our formalism explicitly allows for Γ to have a non-axisymmetric dependence on $\boldsymbol{k}$, which accommodates a bulk flow that is not oriented along the mean magnetic field, as in the case of the solar wind.

As an example, we considered this time-displaced FLRW for the noisy RMHD model, a synthetic model of transverse magnetic turbulence that specifies a power spectrum designed to be similar to the results of dynamical RMHD simulations, and allows scaling to vary the Kubo number $R = (b/B_0)(\ell_\parallel/\ell_\perp)$. For simplicity, we specified a dynamical correlation with no bulk flow, i.e., working in the plasma frame. We examined the mean dynamical correlation, which is the normalized Eulerian time correlation function, and the time-displaced FLRW.

The Eulerian time correlation $\bar{\Gamma}(t)$ that we constructed exhibits different behavior for low or high Kubo number R. For $R \lesssim 1$, $\bar{\Gamma}(t)$ oscillates with decreasing amplitude for increasing t, due to the wave term in the dynamical correlation. This behavior is partly due to power spectrum used for noisy RMHD

with a sharp cutoff at $|k_z| = K$. For $R > 1$, $\bar{\Gamma}(t)$ tends to zero more steadily with increasing t, due to the nonlinear term and (to a lesser extent) the sweeping term.

This was then used to calculate the time-differenced field line diffusion coefficient $D_X(z, t)$ in comparison with its asymptotic limit (at high t) of $2D_x(z)$, where D_x denotes the single-field line diffusion coefficient. At $R > 1$ it was previously found that $2D_x(z)$ rises to a nearly constant value, relatively rapidly with z (Ruffolo & Matthaeus 2013). Here, because the dynamical correlation steadily tends to zero as a function of time difference t, we found that $D_X(z, t)$ steadily rises toward the asymptotic limit $2D_x(z)$ as a function of t. Then at $R < 1$, the asymptotic limit itself oscillates as a function of z, which is again behavior associated with the sharp cutoff at $|k_z| = K$. Furthermore, $D_X(z, t)$ oscillates with both z and t, where the oscillation with t is due to the oscillation of the dynamical correlation. It is interesting that D_X can overshoot its asymptotic limit of $2D_x$ when the dynamical correlation is negative, so that D_X expresses the difference between anticorrelated FLRWs, whereas $2D_x$ expresses the difference between uncorrelated FLRWs. The oscillations decrease with increasing t and z so that D_X tends to a steady asymptotic value.

The oscillations reported here can be attributed to the sharp cutoff in the power spectrum at $|k_z| = K$ for the assumed boxcar profile. While the spectrum from a dynamical RMHD simulation would not have an exact boxcar profile, it is commonly found or expected to rapidly decline for $|k_z|$ above the "critical balance" limit in $\boldsymbol{k}$-space where the Alfvén time equals the nonlinear time. A rapid decline or cutoff in k_z has been found in dynamical RMHD simulations (e.g., Oughton et al. 2004; Snodin et al. 2013b) and is a feature of the theory of Goldreich & Sridhar (1995) and numerous others that invoke critical balance. A sufficiently rapid decline in k_z also leads to the oscillatory behavior in the FLRW, as Snodin et al. (2013b) found for dynamical RMHD simulations.

Our results indicate a dichotomy in the t-dependence of the mean dynamical correlation and the time-differenced field line diffusion coefficient, which is oscillatory (with decorrelation dominated by the wave term) at $R \lesssim 1$ and non-oscillatory (with decorrelation dominated by the nonlinear term) at $R \gtrsim 1$. This coincides with the classic dichotomy in the FLRW, with quasilinear behavior at $R \lesssim 1$ (Jokipii & Parker 1968; Isichenko 1991a) and non-quasilinear behavior at $R \gtrsim 1$, the precise nature of which has been and still is debated (Kadomtsev & Pogutse 1979; Isichenko 1991b; Matthaeus et al. 1995; Vlad et al. 1998; Ruffolo & Matthaeus 2013; Sonsrettee et al. 2015). In the context of the noisy RMHD model, the quasilinear regime involves z-oscillations and the non-quasilinear regime does not. Note that the FLRW studies cited above considered static magnetic fluctuations, so it is fascinating to see the dichotomy in dynamical effects as well. Our predictions could be tested by numerical simulations, analogous to those of Zimbardo et al. (1995) and Giacalone & Jokipii (1999), with a suitable time dependence.

Physically, for the FLRW the quasilinear regime indicates an extrinsic FLRW that decorrelates mainly due to B_0, relative to a distance $\ell_\parallel$, and the non-quasilinear regime has an intrinsic FLRW that decorrelates due to the FLRW itself, due to the action of b over a distance $\ell_\perp$. The comparison between those effects explains the dependence on $R = (b/B_0)(\ell_\parallel/\ell_\perp)$. Meanwhile, the dynamical decorrelation at low R is dominated by effects of Alfvén waves, when the Alfvén timescale, i.e., $1/(k_z v_A)$ for a characteristic wavenumber $k_z \sim 1/\ell_\parallel$, is shorter than the nonlinear timescale $\tau_0 = \ell_\perp/u_\perp$. Assuming equipartition between magnetic and velocity fluctuations, these timescales are equal at $R = 1$. This is why the transition between the types of t-dependence in our results occurs at $R \sim 1$ in coincidence with the transition in FLRW behavior as a function of z.

Our work is relevant to a variety of astrophysical situations. In particular, dynamical RMHD models are frequently applied to the solar corona and coronal magnetic loops. The rate of change of magnetic connectivity is directly related to the rate of interchange reconnection at the boundaries of coronal loops, which is a popular model to explain the origin and coronal loop-like properties of plasma in the classical slow solar wind (e.g., Rappazzo et al. 2012, and references therein). It is in fact the process of continuously changing connectivity near the boundary of coronal holes that originally motivated the present work. In addition, previous work on the width of filaments within coronal loops due to the spread of electrons from heating sites (Galloway et al. 2006), which involved the FLRW, could be extended to consider time-dependent spreading from transient heating events. In one view, moss emission in the solar transition region is attributed to magnetic connectivity from sites of heating in the overlying hot coronal loops (Kittinaradorn et al. 2009), so this work could provide a basis to examine the dynamics of moss emission and test the validity of this view of the origin of moss emission.

For more general types of turbulent fluctuations, the time-differenced FLRW, as defined and calculated in the present work, is directly relevant to observations at a fixed spacecraft position of plasma and energetic particles, which often closely follow magnetic field lines in space. This idea may also be applied looking *backward*, asking whether the spacecraft is magnetically connected to a specific source region, and how that connectivity may change as a function of time. Source regions of interest include the Earth's bow shock during upstream events, other shocks that accelerate energetic particles and modify plasma properties, the source region of solar energetic particles, and reconnection regions that allow access to other plasma and particle populations. The ensemble average statistics discussed in the present work provide part of the answer. Another part comes from the study of conditional statistics, which depend on the source or observer location with respect to intermittent turbulence structure. This includes temporary topological trapping, in which some magnetic field lines and energetic particles along those field lines are temporarily confined to flux structures (Ruffolo et al. 2003; Chuychai et al. 2005, 2007; Tooprakai et al. 2007; Seripienlert et al. 2010), which can explain observed dropouts in energetic particles from impulsive solar events (Mazur et al. 2000; Gosling et al. 2004), indicating that such trapping can persist in the interplanetary medium over a distance of 1 AU. Such effects of the small-scale turbulence topology continue to be an important subject of inquiry to complement ensemble average statistics as examined in the present work.

As a final remark, we emphasized that time dependent changes of connectivity, treated statistically here, may often be realized in nature through frequent small scale random component reconnection events, as described in Rappazzo et al. (2012). The theoretical framework we presented here aims to capture the effects of many such reconnection events as an intrinsic part of the evolution of the turbulent system. When

such a situation occurs, the mean properties of the reconnection events will be governed by turbulence time scales (e.g., Servidio et al. 2010) and thus the relatively simple formulation we presented here may become relevant, without a need to compute properties of any individual reconnection event. Detailed comparisons with simulations and observations that are beyond the scope of the present theoretical treatment will be needed to assess whether this approach is effective.

This work was partially supported by the Thailand Research Fund, the U.S. NSF (AGS-1063439 and SHINE AGS-1156094), NASA (Heliophysics Theory NNX11AJ44G), and the Solar Probe Plus/ISIS project.

APPENDIX
OTHER CLOSURE MODELS

Section 2.4 described a closure model (RBD) for σ_x^2, σ_X^2, and σ_Y^2 in theories for the FLRW and time-differenced FLRW. For completeness, in this appendix we describe two other closure models, which have some deficiencies that make them less appropriate than RBD for the time-differenced FLRW.

A.1 Self-closure

Self-closure identifies σ_x^2 with $\langle x^2\rangle$, and in this case, also σ_X^2 with $\langle X^2\rangle$. This technique was developed and studied for use with Corrsin's approximation in other physical situations (Saffman 1963; Taylor & McNamara 1971; Lundgren & Pointin 1976) and has more recently been applied to study magnetic field lines (Wang et al. 1995; Shalchi & Kourakis 2007; Snodin et al. 2013a). While this is self-consistent, it is sometimes less accurate (in comparison with direct computer simulations) than simpler closure models for FLRW problems (Snodin et al. 2013b), presumably because any approximation errors at low Δz are amplified by the self-consistent procedure. For simplicity in this section we demonstrate our points for the case that $\Gamma(\boldsymbol{k}, t)$ is axisymmetric in the k_x–k_y plane, so $\langle X^2\rangle = \langle Y^2\rangle$ and $\sigma_X^2 = \sigma_Y^2$.

Direct substitution for σ_x^2 and σ_X^2 in Equations (17) and (18) yields

$$\left\langle X^2(z,t)\right\rangle = \frac{4}{B_0^2}\int_0^z\int_0^{z-z'}\int\int S_{xx}(\boldsymbol{k})e^{ik_z\Delta z}e^{-k_\perp^2\left\langle x^2(\Delta z)\right\rangle/2} \times\left[1-\Gamma_\pm(\boldsymbol{k},t)e^{-k_\perp^2\left\langle X^2(z',t)\right\rangle/2}\right] \times d\boldsymbol{k}_\perp dk_z d\Delta z dz' \tag{44}$$

$$\left\langle x^2(z)\right\rangle = \frac{2}{B_0^2}\int_0^z\int_0^{z-z'}\int\int S_{xx}(\boldsymbol{k})e^{ik_z\Delta z}e^{-k_\perp^2\left\langle x^2(\Delta z)\right\rangle/2} \times d\boldsymbol{k}_\perp dk_z d\Delta z dz'. \tag{45}$$

Note that these coupled equations are nonlocal in the sense that the right hand side depends on $\langle x^2(\Delta z)\rangle$ for $0 \leqslant \Delta z \leqslant z$ and on $\langle X^2(z', t)\rangle$ for $0 \leqslant z' \leqslant z$.

As noted in the work cited above, Equation (45) for the FLRW can be converted into a second-order ODE; however, Equation (44) for the time-differenced FLRW does not yield an ODE in an analogous way. To show this, let us use the simplified notation of Equations (2) and (8),

$$\left\langle x^2(z)\right\rangle = \frac{2}{B_0^2}\int_0^z\int_0^{z-z'}\mathcal{L}_{xx}(\Delta z)d\Delta z dz' \tag{46}$$

$$\left\langle X^2(z,t)\right\rangle = \frac{4}{B_0^2}\int_0^z\int_0^{z-z'}[\mathcal{L}_{xx}(\Delta z) - \mathcal{L}_{xx}(\Delta z, z', t)]d\Delta z dz', \tag{47}$$

use the variables $v \equiv \langle x^2\rangle$ (variance) and $D \equiv (1/2)(dv/dz)$ (running diffusion coefficient), and differentiate v twice:

$$\frac{dv}{dz} = 2D(z), \tag{48}$$

where

$$D(z) = \frac{1}{B_0^2}\int_0^z \mathcal{L}_{xx}(\Delta z)d\Delta z \tag{49}$$

and

$$\frac{dD}{dz} = \frac{1}{B_0^2}\mathcal{L}_{xx}(z) = \frac{1}{B_0^2}\int\int S_{xx}(\boldsymbol{k})e^{ik_z z}e^{-k_\perp^2 v(z)/2}d\boldsymbol{k}_\perp dk_z. \tag{50}$$

Equations (48) and (50) represent coupled 1st-order ODEs for the FLRW, which are equivalent to a 2nd-order ODE. When we attempt an analogous derivation for the time-differenced FLRW, we define $V(z|t) \equiv \langle X^2(z, t)\rangle$ and obtain

$$\frac{dV}{dz} = 4D(z) - 4C(z|t), \tag{51}$$

where

$$C(z|t) \equiv \frac{1}{B_0^2}\int_0^z \mathcal{L}_{xx}(z - z', z', t)dz'. \tag{52}$$

The problem is that on the right hand side, z appears both as the limit of integration and in an argument of $\mathcal{L}_{xx}$, so that

$$\frac{dC}{dz} = \frac{1}{B_0^2}\mathcal{L}_{xx}(0, z, t) + \frac{1}{B_0^2}\int_0^z \frac{d}{dz}\mathcal{L}_{xx}(z - z', z', t)dz'. \tag{53}$$

That integral involves $v(z - z')$ and $D(z - z')$ for $0 \leqslant z - z' \leqslant z$ and $V(z', t)$ for $0 \leqslant z' \leqslant z$, so we obtain an integro-differential equation instead of an ODE.

The equations of the time-differenced FLRW with self-closure are quite cumbersome in comparison with the other closure models, and we do not make use of self-closure for the example calculations in this work.

A.2 Diffusive Decorrelation

DD is another closure method for the FLRW and analogous problems (Salu & Montgomery 1977; Matthaeus et al. 1995) in which $\sigma_x^2(z)$ is set to $2D_\infty z$, based on the high-z diffusive behavior of $\langle x^2\rangle$. DD has been widely used in Corrsin-based calculations of the FLRW (Matthaeus et al. 1995; Ruffolo et al. 2006; Shalchi 2009, and references therein) and field line separation (Ruffolo et al. 2004). The DD closure for the FLRW

can be expressed as

$$D_\infty \equiv \lim_{z\to\infty}\frac{1}{2}\frac{d\left\langle x^2\right\rangle}{dz} = \frac{1}{B_0^2}\int_0^\infty \mathcal{L}_{xx}(\Delta z)d\Delta z = \frac{1}{B_0^2}\int_0^\infty \int\int S_{xx}(\boldsymbol{k})e^{ik_z\Delta z}e^{-k_\perp^2 D_\infty \Delta z}d\boldsymbol{k}_\perp dk_z d\Delta z = \frac{1}{B_0^2}\int\int \frac{S_{xx}(\boldsymbol{k})}{k_\perp^2 D_\infty - ik_z}d\boldsymbol{k}_\perp dk_z. \quad (54)$$

Because the integrand undergoes complex conjugation as $\boldsymbol{k}\to-\boldsymbol{k}$, we can use the real part alone:

$$D_\infty = \frac{1}{B_0^2}\int\int \frac{k_\perp^2 D_\infty}{k_\perp^4 D_\infty^2 + k_z^2}S_{xx}(\boldsymbol{k})d\boldsymbol{k}_\perp dk_z. \quad (55)$$

Once D_∞ has been obtained from this implicit equation, the closure can be used in Equation (18) for any z:

$$\left\langle x^2(z)\right\rangle = \frac{2}{B_0^2}\int_0^z\int_0^{z-z'}\int\int S_{xx}(\boldsymbol{k}) \times e^{ik_z\Delta z}e^{-k_\perp^2 D_\infty\Delta z}d\boldsymbol{k}_\perp dk_z d\Delta z dz' = \frac{2z}{B_0^2}\int\int \frac{S_{xx}(\boldsymbol{k})}{k_\perp^2 D_\infty - ik_z} \times\left[1 - g\left(k_\perp^2 D_\infty z - ik_z z\right)\right]d\boldsymbol{k}_\perp dk_z, \quad (56)$$

where $g(u)\equiv(1-e^{-u})/u$. Note that $g(u)\approx 1$ for $|u|\ll 1$ and declines to zero as $\mathrm{Re}(u)\to\infty$. Here g is significantly non-zero only for $k_\perp \lesssim (D_\infty z)^{-1/2}$, which becomes a smaller region with decreasing effect on the integral as $z\to\infty$, in which case Equation (56) becomes consistent with Equation (55). It is straightforward to show that the short-distance limit of Equation (56) is consistent with Equation (25).

The extension to use DD for the time-differenced FLRW is straightforward because in the long-distance limit, the field lines at different times become uncorrelated at long distances, where the random walks are independent due to their relative perpendicular displacement, except in the case that the magnetic fluctuations depend only on z (slab fluctuations). Setting aside that special case, the long-distance limit for $t\neq 0$ is $\langle X^2(z,t)\rangle \to 2\langle x^2(z)\rangle = 4D_\infty z$. Then setting $\sigma_X^2 = 4D_\infty z$, Equation (17) becomes

$$\left\langle X^2(z,t)\right\rangle = \frac{4z}{B_0^2}\int\int \frac{S_{xx}(\boldsymbol{k})}{k_\perp^2 D_\infty - ik_z} \times\left\{1 - g\left(k_\perp^2 D_\infty z - ik_z z\right) - \Gamma_\pm(\boldsymbol{k},t)\left[g\left(2k_\perp^2 D_\infty z\right) - e^{-\left(k_\perp^2 D_\infty - ik_z\right)z} \times g\left(k_\perp^2 D_\infty z + ik_z z\right)\right]\right\}d\boldsymbol{k}_\perp dk_z. \quad (57)$$

It is straightforward to show that the long-distance limit of Equation (57) is $\langle X^2(z,t)\rangle = 4D_\infty z$, as expected, and the short-distance limit is consistent with Equation (26).

However, the simplicity of using $\sigma_X^2(z,t) = 4D_\infty z$ for any time t is also a significant drawback to the use of DD for the time-differenced FLRW. This form fails to take the dynamics into account. One would expect that $\sigma_X^2(z,t)$ should depend on t, and indeed that it tends to zero as $t\to 0$ for any z. For this reason, we do not consider DD to be a physically appropriate closure for the time-differenced FLRW.

REFERENCES

Batchelor, G. K. 1950, QJRMS, 76, 133
Belcher, J. W., & Davis, L., Jr. 1971, JGR, 76, 3534
Bieber, J. W., Matthaeus, W. H., Smith, C. W., et al. 1994, ApJ, 420, 294
Chandran, B. D. G., & Cowley, S. C. 1998, PhRvL, 80, 3077
Chen, S., & Kraichnan, R. H. 1989, PhFl, A1, 2019
Chuychai, P., Ruffolo, D., Matthaeus, W. H., & Meechai, J. 2007, ApJ, 659, 1761
Chuychai, P., Ruffolo, D., Matthaeus, W. H., & Rowlands, G. 2005, ApJL, 633, L49
Corrsin, S. 1959, in Atmospheric Diffusion and Air Pollution, Vol. 6, ed. F. Frenkel & P. Sheppard (New York: Academic), 161
Dmitruk, P., Gómez, D. O., & DeLuca, E. E. 1998, ApJ, 505, 974
Frisch, U. 1995, Turbulence. The Legacy of A.N. Kolmogorov (Cambridge: Cambridge Univ. Press)
Galloway, R. K., Helander, P., & MacKinnon, A. L. 2006, ApJ, 646, 615
Ghilea, M. C., Ruffolo, D., Chuychai, P., et al. 2011, ApJ, 741, 16
Giacalone, J., & Jokipii, J. R. 1999, ApJ, 520, 204
Goldreich, P., & Sridhar, S. 1995, ApJ, 438, 763
Gosling, J. T., Skoug, R. M., McComas, D. J., & Mazur, J. E. 2004, ApJ, 614, 412
Hesse, M., Birn, J., & Schindler, K. 1990, JGR, 95, 6549
Isichenko, M. B. 1991a, PPCF, 33, 795
Isichenko, M. B. 1991b, PPCF, 33, 809
Jokipii, J. R. 1966, ApJ, 146, 480
Jokipii, J. R. 1973, ApJ, 183, 1029
Jokipii, J. R., & Parker, E. N. 1968, PhRvL, 21, 44
Kadomtsev, B. B., & Pogutse, O. P. 1979, in Proc. 7th Int. Conf. 649, Plasma Physics and Controlled Nuclear Fusion Research 1978 (Vienna: IAEA)
Kinney, R., & McWilliams, J. C. 1998, PhRvE, 57, 7111
Kittinaradorn, R., Ruffolo, D., & Matthaeus, W. H. 2009, ApJL, 702, L138
Kolmogorov, A. 1941, DoSSR, 30, 301
Kraichnan, R. H. 1966, PhFl, 9, 1937
Lazarian, A. 2006, ApJL, 645, L25
Lazarian, A., & Vishniac, E. T. 1999, ApJ, 517, 700
Lundgren, T. S. 1981, JFM, 111, 27
Lundgren, T. S., & Pointin, Y. B. 1976, PhFl, 19, 355
Matthaeus, W. H., & Bieber, J. W. 1999, in AIP Conf. Proc. 471, Solar Wind Nine, ed. S. Habbal, R. Esser, J. V. Hollweg & P. A. Isenberg (Woodbury: AIP), 515
Matthaeus, W. H., Bieber, J. W., Ruffolo, D., Chuychai, P., & Minnie, J. 2007, ApJ, 667, 956
Matthaeus, W. H., Ghosh, S., Oughton, S., & Roberts, D. A. 1996, JGR, 101, 7619
Matthaeus, W. H., Gray, P. C., Pontius, D. H., Jr., & Bieber, J. W. 1995, PhRvL, 75, 2136
Matthaeus, W. H., Qin, G., Bieber, J. W., & Zank, G. 2003, ApJL, 590, L53
Mazur, J. E., Mason, G. M., Dwyer, J. R., et al. 2000, ApJL, 532, L79
Montgomery, D. 1982, PhST, 1, 83
Narayan, R., & Medvedev, M. V. 2001, ApJL, 562, L129
Newcomb, W. A. 1958, AnPhy, 3, 347
Oughton, S., Dmitruk, P., & Matthaues, W. H. 2004, PhPl, 11, 2214
Oughton, S., Dmitruk, P., & Matthaues, W. H. 2006, PhPl, 13, 042306
Oughton, S., Matthaeus, W. H., Dmitruk, P., et al. 2001, ApJ, 551, 565
Perez, J. C., & Chandran, B. D. G. 2013, ApJ, 776, 124
Pommois, P., Veltri, P., & Zimbardo, G. 2001, PhRvE, 63, 066405
Ragot, B. R. 2008, ApJ, 682, 1416
Rappazzo, A. F., Matthaeus, W. H., Ruffolo, D., Servidio, S., & Velli, M. 2012, ApJL, 758, L14
Rechester, A. B., & Rosenbluth, M. M. 1978, PhRvL, 40, 38
Richardson, L. F. 1926, RSPSA, 110, 709
Ruffolo, D., Chuychai, P., & Matthaeus, W. H. 2006, ApJ, 644, 971
Ruffolo, D., & Matthaeus, W. H. 2013, PhPl, 20, 012308
Ruffolo, D., Matthaeus, W. H., & Chuychai, P. 2003, ApJL, 597, L169

Ruffolo, D., Matthaeus, W. H., & Chuychai, P. 2004, ApJ, 614, 420
Ruffolo, D., Pianpanit, T., Matthaeus, W. H., & Chuychai, P. 2012, ApJL, 747, L34
Saffman, P. G. 1963, ApScR, A11, 245
Salu, Y., & Montgomery, D. C. 1977, PhFl, 20, 1
Seripienlert, A., Ruffolo, D., Matthaeus, W. H., & Chuychai, P. 2010, ApJ, 711, 980
Servidio, S., Matthaeus, W. H., Shay, M. A., et al. 2010, PhPl, 17, 032315
Servidio, S., Matthaeus, W. H., Wan, M., et al. 2014, ApJ, 785, 56
Shalchi, A. 2009, Nonlinear Cosmic Ray Diffusion Theories (Berlin: Springer)
Shalchi, A., Bieber, J. W., Matthaeus, W. H., & Schlickeiser, R. 2006, ApJ, 642, 230
Shalchi, A., & Hussein, M. 2014, ApJ, 794, 56
Shalchi, A., & Kourakis, I. 2007, PhPl, 14, 092903
Snodin, A. P., Ruffolo, D., & Matthaeus, W. H. 2013a, ApJ, 762, 66
Snodin, A. P., Ruffolo, D., Oughton, S., Servidio, S., & Matthaeus, W. H. 2013b, ApJ, 779, 56
Sonsrettee, W., Subedi, P., Ruffolo, D., et al. 2015, ApJ, 798, 59
Strauss, H. R. 1976, PhFl, 19, 134
Taylor, J. B., & McNamara, B. 1971, PhFl, 14, 1492
Tooprakai, P., Chuychai, P., Minnie, J., et al. 2007, GRL, 34, L17105
Vlad, M., Spineanu, F., Misguich, J. H., & Balescu, R. 1998, PhRvE, 58, 7359
Wang, H.-D., Vlad, M., Vanden Eijnden, E., et al. 1995, PhRvE, 51, 4844
Weygand, J. M., Matthaeus, W. H., Kivelson, M. G., & Dasso, S. 2013, JGR, 118, 3995
Zank, G. P., & Matthaeus, W. H. 1992, JPlPh, 48, 85
Zaslavsky, G. M., & Chirikov, B. V. 1972, SvPhU, 14, 549
Zhou, Y., Matthaeus, W. H., & Dmitruk, P. 2004, RvMP, 76, 1015
Zimbardo, G., Veltri, P., Basile, G., & Principato, S. 1995, PhPl, 2, 2653